



OPEN

## BUB1 induces AKT/mTOR pathway activity to promote EMT induction in human small cell lung cancer

Moufeng Wang<sup>1,2,3</sup>, Lijie You<sup>3</sup>, Zhixiong Su<sup>3</sup>, Yufang He<sup>3</sup>, Deyu Li<sup>3</sup>✉ & Zhenhua Liu<sup>3</sup>✉

Small cell lung cancer (SCLC) is a very aggressive tumor. Abnormal expression of BUB1 has been reported in several cancer types, wherein it plays a range of functional roles. This work aimed to elucidate the functional significance and molecular impacts of BUB1 in SCLC. It was found that SCLC cell lines exhibited significant BUB1 upregulation relative to control bronchial cells using data from the Gene Expression Omnibus (GEO) database and verified by immunohistochemical staining. BUB1 was also found to promote the proliferative, migratory, invasive activity of SCLC cells, as shown by CCK-8, 3D migration wound-healing, and Transwell assays, as well as flow cytometry. Additionally, it was found that BUB1 silencing enhanced E-cadherin expression while suppressing N-cadherin, Vimentin, ZEB-1, and Snail levels, as shown by Western immunoblotting. The loss of BUB1 also reduced p-AKT and p-mTOR levels without altering total AKT or mTOR protein levels. In conclusion, BUB1 functions as an oncogenic promoter in SCLC, potentially regulating the epithelial-mesenchymal transition by activation of AKT/mTOR signaling.

**Keywords** BUB1, AKT/mTOR, EMT, Small cell lung cancer

Lung cancer is a prevalent and potentially fatal form of cancer throughout the world<sup>1</sup>. Approximately 15% of all lung cancer cases can be attributed to small cell lung cancer (SCLC)<sup>2</sup>. SCLC tumors tend to be highly aggressive, such that 70% of patients present with advanced disease, exhibiting a median survival of under 1 year<sup>3</sup>. Progress in the treatment of SCLC has been relatively limited in recent years, with chemotherapy having emerged as a mainstay of patient treatment four decades ago. While such treatment can initially yield positive outcomes in SCLC patients, most ultimately develop chemoresistant disease after a short remission. Immunotherapy has provided a promising opportunity to treat SCLC patients better, but first-line immunotherapy outcomes have unfortunately failed to achieve overall response rates higher than those of chemotherapy<sup>4-7</sup>. Further work is thus needed to clarify SCLC's pathogenesis and define novel targets for treating affected patients.

The serine/threonine kinase BUB1 is an essential component of the spindle assembly checkpoint (SAC) assembly crucial in chromosome segregation<sup>8</sup>. Abnormal BUB1 expression has been detected in several cancer types. For example, Jiang et al. noted that BUB1 promoted bladder tumorigenesis and progression through its ability to regulate STAT3<sup>9</sup>. High BUB1 expression levels have also been detected in osteosarcoma<sup>10</sup> and hepatocellular carcinoma<sup>11</sup>, with BUB1 silencing suppressing tumors' growth, migratory activity, and invasivity. However, BUB1 has also been found to correlate negatively with the overall survival of low-grade breast<sup>12</sup> and gastric cancer<sup>13</sup> patients. Lower BUB1 levels have also been linked to aneuploidy and tumorigenesis<sup>14</sup>. As such, BUB1 exhibits contrasting oncogenic roles that appear to be tumor-type-dependent. The function of BUB1 in SCLC has yet to be established.

Here, significant increases in BUB1 expression were observed in SCLC, prompting further inquiries to clarify the effect of BUB1 knockdown, overexpression, and pharmacological inhibition on the invasive, migratory, and survival characteristics of SCLC cells, with corresponding analyses of the underlying molecular mechanisms. These analyses ultimately demonstrated that BUB1 may promote AKT/mTOR pathway activation, thus promoting SCLC's growth and metastatic progression.

<sup>1</sup>Department of Oncology, The First Affiliated Hospital of Fujian Medical University, No. 20 Chazhong Road, Fuzhou 350005, Fujian, China. <sup>2</sup>Department of Oncology, National Regional Medical Center, Binhai Campus of the First Affiliated Hospital, Fujian Medical University, Fuzhou 350212, Fujian, China. <sup>3</sup>Department of Oncology, Shengli Clinical Medical College of Fujian Medical University, Fujian Provincial Hospital, Fuzhou University Affiliated Provincial Hospital, Fuzhou 350001, Fujian, China. ✉email: ahu1982@163.com; liuzhenhua6909@163.com

## Materials and methods

### Tissue specimens

A total of 21 paired samples of SCLC and normal tissue were acquired from patients at Fujian Provincial Hospital, with verified clinical and histological diagnoses. The Accreditation Committee of Fujian Provincial Hospital has approved all experiments involving human samples (Ethics approval number: 2020-016-03). All experiments were performed in accordance with relevant guidelines and regulations.

### Immunohistochemistry

The immunohistochemical (IHC) staining was conducted through probing slides with primary anti-BUB1 (Cat. No. ab 195,268, Abcam, USA) overnight at 4 °C and incubating with secondary antibodies for 30 min at room temperature. After that, these sections were stained for 10 min using DAB staining. Tumor staining positivity rates were graded as 1 (0–25%), 2 (25–50%), 3 (51–75%), and 4 (76–100%). BUB1 staining intensity levels were evaluated as 0 (negative), 1 (weak), 2 (moderate), or 3 (strong). Immunoreactive score (IRS) values were computed semiquantitatively by multiplying these two scores. Two pathologists were responsible for reviewing all tissue sections.

### Cell culture

The NCI-H446, SBC-2, H69AR, and DMS114 human SCLC cell lines and the 16HBE control human bronchial epithelial cells were procured from the American Type Culture Collection (ATCC) located in Virginia, USA. The cells were cultured in RPMI-1640 medium supplemented with 10% fetal bovine serum (Gibco, USA) at 37 °C and a CO<sub>2</sub> concentration of 5% in an incubator. Monthly assessments were conducted to ensure the absence of mycoplasma contamination.

### BUB1 silencing

BUB1-specific siRNA constructs were synthesized by Zaiji Co. Ltd. (Fuzhou, China) with the primer sequences as given below:

siRNA-1 sense 5'-AGGAAAGGUCCGAGGUUAATT-3',  
antisense 5'-UUAACCUCGGACCUUCCUTT-3';  
siRNA-2 sense 5'-UGACAAAGAUGAAUGGCAATT-3',  
antisense 5'-UUGCCAUUCAUCUUUGUCATT-3'.

In addition, negative control siRNA (si-NC; sense: 5'-UUCUCCGAACGUGUCACGUTT-3', antisense: 5'-ACGUGACACGUUCGGAGAATT-3') was obtained.

SBC-2 and NCI-H446 cell lines were cultured in 6-well plates until reaching a confluency of 30–50%. Lipofectamine 3000 (Invitrogen, USA) was then employed to transfect these cells with si-NC or si-BUB1 constructs. Subsequently, the medium was replaced after 6 h.

### BUB1 overexpression and mTOR inhibitor

Lentivirus-BUB1 was constructed by Genechem (Shanghai, China). The SBC-2 and NCI-H446 cell lines were transfected with the lentivirus according to the manufacturer's instructions.

To further determine the effects of BUB1 on the mTOR pathway, the transfected cells were seeded in 10-cm plates (1 × 10<sup>6</sup> cells per plate) and treated with the control solution or mTOR inhibitor, Everolimus (1 μmol/L) (MCE, China).

### Pharmacological inhibition of BUB1

SBC-2 and NCI-H446 cells were incubated with 1.4 μM BAY 1,816,032 (an inhibitor of BUB1) (MCE) or DMSO<sup>15</sup>.

### qPCR

The extraction of total cellular RNA was performed using Nucleozol (MN, Germany), followed by the synthesis of complementary DNA (cDNA) from 1 μg of total RNA using a cDNA kit (Takara, Japan) according to the instructions supplied by the manufacturer. The qPCR analyses were performed using the Step One Plus™ Real-Time PCR System (Thermo Fisher Scientific, MA, USA), utilizing the default thermocycler and software configurations. GAPDH/U6 was used to normalize relative gene expression, assessed via the 2<sup>-ΔΔCT</sup> method.

### Western immunoblotting

Cellular proteins were extracted using RIPA buffer (Solarbio, Beijing, China) that contained protease inhibitors. Protein concentrations were then measured using the BCA reagent (Beyotime, Beijing, China). The samples were subsequently subjected to separation using SDS-PAGE and afterward transferred onto PVDF membranes (Millipore). The blots were cut prior to hybridisation with antibodies. These blots were blocked for 2 h with 5% non-fat milk before overnight incubation with primary antibodies against the following antigens at 4 °C: BUB1 (ab 195268, Abcam, USA), p-mTOR (ab109268, Abcam), mTOR (ab 134903, Abcam), AKT (60203-2-Ig, Proteintech, China), p-AKT (80455-1-RR, Proteintech), Snail (13099-1-AP, Proteintech), β-Actin (Cat No. ab 8226, Abcam), Vimentin (10366-1-AP, Proteintech), N-cadherin (22018-1-AP, Proteintech), E-cadherin (20874-1-AP, Proteintech), and Zeb-1 (21544-1-AP, Proteintech). Blots were then rinsed thrice with TBST, probed for 50 min with secondary antibodies, and blots were quantitatively imaged with ImageJ 8.0. β-actin served as a loading control.

### Cell viability assay

After the cells had been cultured for 24, 48, 72, 96, or 120 h, they were transferred to 96-well plates ( $2 \times 10^3$ /well), and 10  $\mu$ L of CCK-8 reagent (Dojindo, Kumamoto, Japan) was added to each well. Each well's absorbance at 450 nm was measured after 2 h at 37 °C of incubation. The resulting data was then used for developing a viability curve.

### Tumor sphere proliferation assay

The proper quantity of 200  $\mu$ L was applied to the wells of round-bottom ultra-low-attachment 96-well plates (Corning, USA) after suitably transfected SCLC cells were suspended at  $2 \times 10^4$ . Plates were centrifuged for 3 min ( $300 \times g$ , 4 °C) to ensure the central location of spheroids in these wells<sup>16</sup>. Following a 5-days incubation period, the resultant tumor spheres were imaged, and the diameter of each was measured. Tumor sphere proliferation curves were then generated based on the rate of diameter change and time.

### Cell cycle assay

The progression through the cell cycle was examined using a cell cycle test kit (Cat. no. MA0334, Dalian Meilun Biotechnology Co. Ltd., China). Cells were extracted 48 h after transfection, washed with PBS, fixed in 75% ethanol for 24 h at 4 °C, suspended in cold PBS, and stained with RNase A and propidium iodide (PI). ModFit v 5.0 (Verity Software House, ME, USA) assessed cells in different cell cycle phases.

### Wound healing assay

In wound healing assay, tumor cells were transferred into 6-well plates ( $5 \times 10^5$ /well) and cultured until 95% confluence to examine migratory activity. A micropipette tip was used to create a scratch in the monolayer, and the wound was evaluated at 0, 24, and 48 h after the wound appeared using a light microscope. Wound healing rate (%) was then calculated as (area at 0 h—area at 24 or 48 h) / area at 0 h  $\times$  100%. All analyses were repeated in triplicate.

### 3D migration assay

The proper quantity of 200  $\mu$ L was applied to the wells of round-bottom ultra-low-attachment 96-well plates (Corning, USA) after suitably transfected SCLC cells were suspended at  $2 \times 10^4$ . Plates were centrifuged for 3 min ( $300 \times g$ , 4 °C) to ensure the central location of spheroids in these wells<sup>16</sup>. Cells were then incubated in the tissue culture incubator to enable sphere formation, after which these spheres were carefully transferred onto 6-well plates that had been pre-coated using 0.1% gelatin. The migratory area for each sphere was imaged and quantified, with the resultant measurements normalized to the initial sphere area. The rates of migration change over time were then utilized to generate 3D migration curves.

### Transwell assay

Transwell invasion assays were utilized to assess cellular invasion. After dilution with RPMI-1640 at a 1:8 ratio, BD Matrigel™ (BD Biosciences) was added to cold Transwell chambers (pore size: 8  $\mu$ m, Corning, USA) followed by incubation for 2 h at 37 °C. Following cell suspension at a density of  $20 \times 10^4$ /mL, 100  $\mu$ L of the cells were added to the upper chamber of each Transwell insert in serum-free medium, and 700  $\mu$ L of RPMI-1640 with 10% FBS was added to the lower chamber. After being incubated for 48 h, the cells in the upper chamber were counted using an inverted microscope (200 $\times$ ), stained with crystal violet, and fixed with 4% paraformaldehyde for 15 min.

### Zebrafish xenograft assay

Fuzhou Bio-Service Biotechnology Co. Ltd. supplied transgenic zebrafish Tg (fli1:EGFP) (Fuzhou, China). NCI-H446 and SBC-2 cells were transfected with BUB1-specific or control siRNA constructs. The cells were stained using the CM-Dil fluorescent lipophilic dye (Meilun Biotechnology, Dalian, China). After staining, the cells were microinjected into the yolk sac of zebrafish embryos at 48 h post-fertilization (hpf). Each fish received an injection of 300–400 cells using GB100T-8P injection glass capillaries (Science Products GmbH, Hofheim am Taunus, Germany) that were pulled using FemtoJet 4i microinjectors (Eppendorf, Hamburg, Germany). Each experimental group consisted of five fish specimens subjected to incubation at a temperature of 28 °C for 48 h after injection. The imaging procedure was conducted at two-time points, at 0 and 48 h after injection (hpi). A fluorescent stereomicroscope manufactured by Nikon in Tokyo, Japan, was used for this purpose. The assessment of the fluorescent region in each fish was carried out using ImageJ software. The tumor growth rate (%) was calculated as (fluorescent area at 48 hpi—area at 0 hpi) / area at 0 hpi  $\times$  100%.

### Bioinformatics analyses

The GSE30219 and GSE149507 datasets from the GEO database (<http://www.ncbi.nih.gov/geo>) were downloaded, and differential gene expression was assessed with the R limma package. Cancer Cell Line Encyclopedia database data were evaluated with the cancer dependency map (DepMap) tool (<https://depmap.org/portal/>).

### Statistical analysis

The data were analyzed using GraphPad Prism 9.0 and SPSS 25.0 software. Statistical comparisons were performed using Student's t-tests for independent samples or one-way ANOVAs, followed by Fisher's least significant difference test. A significance level of  $P < 0.05$  was selected as the threshold for determining statistical significance.

## Results

### SCLC tumors exhibit BUB1 upregulation

An initial analysis of the GSE30219 dataset revealed significantly elevated BUB1 mRNA levels in SCLCL tumors as compared to normal tissues (Fig. 1A). Consistently, tumor tissues in the GSE149507 dataset expressed higher BUB1 mRNA levels than did matched paracancerous tissue samples (Fig. 1B). When these two datasets were removed after the removal of batch effects, significantly higher BUB1 expression was detected in M1 patients as compared to M0 patients (Fig. 1C), suggesting a possible role for BUB1 in the induction of tumor metastasis. Significantly elevated BUB1 protein levels were additionally detected in the SBC-2, NCI-H446, H69AR, and DMS114 SCLC tumor cell lines than the control 16HBE epithelial cells (Fig. 1D). The NCI-H446 and SBC-2 cell lines, which expressed the highest BUB1 levels, were then selected for downstream experimental use. An IHC approach was additionally utilized to compare BUB1 protein levels in 21 paired SCLC patient samples. These analyses revealed that BUB1 primarily localized to the nuclei of tumor cells (Fig. 1E), with significantly higher IRS scores in the tumor samples than the paracancerous samples.

### Characterization of the in vitro functions of BUB1 in SCLC

To begin investigating the biological functions played by BUB1, the DepMap tool was used to explore datasets corresponding to the expression and CRISPR-mediated knockout of BUB1. Moderately high BUB1 expression was observed in SCLC cell lines in the “Expression” dataset. In contrast, the CRISPR dataset revealed that the knockout of BUB1 impaired the growth of SCLC cell lines (Fig. 2A). Three different siRNA constructs

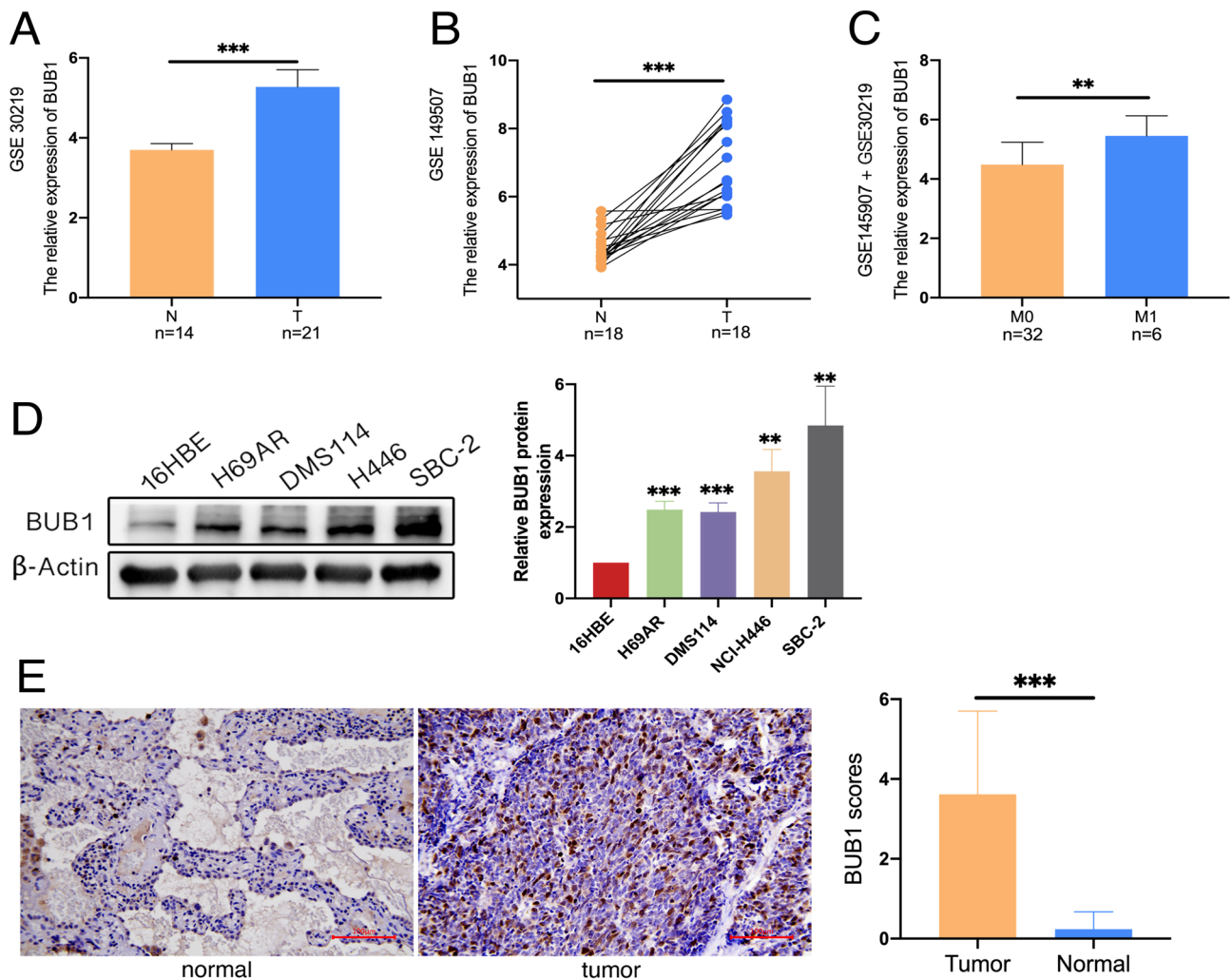


**Fig. 1.** SCLC tumors exhibit high BUB1 expression. (A, B) Levels of BUB1 mRNA in normal tissues and SCLC tumors from the GSE30219 (A) and GSE149507 (B) datasets. (C) After using the R limma package to remove batch effects, the GSE30219 and GSE149507 datasets were merged, and BUB1 mRNA levels were compared between patients without (M0) and with (M1) distant metastases. (D) Western immunoblotting revealed the upregulation of BUB1 in SCLC cell lines (SBC-2, NCI-H446, H69AR, DMS114) as compared to control epithelial cells (16HBE). (E) IHC staining for BUB1 in tumors and paracancerous tissues (200 $\times$ ), revealing significantly higher IRS scores for tumor samples. \*For each experiment, the data are expressed as means  $\pm$  SD (n = 3). \* $P < 0.05$ , \*\* $P < 0.01$ , \*\*\* $P < 0.001$ .

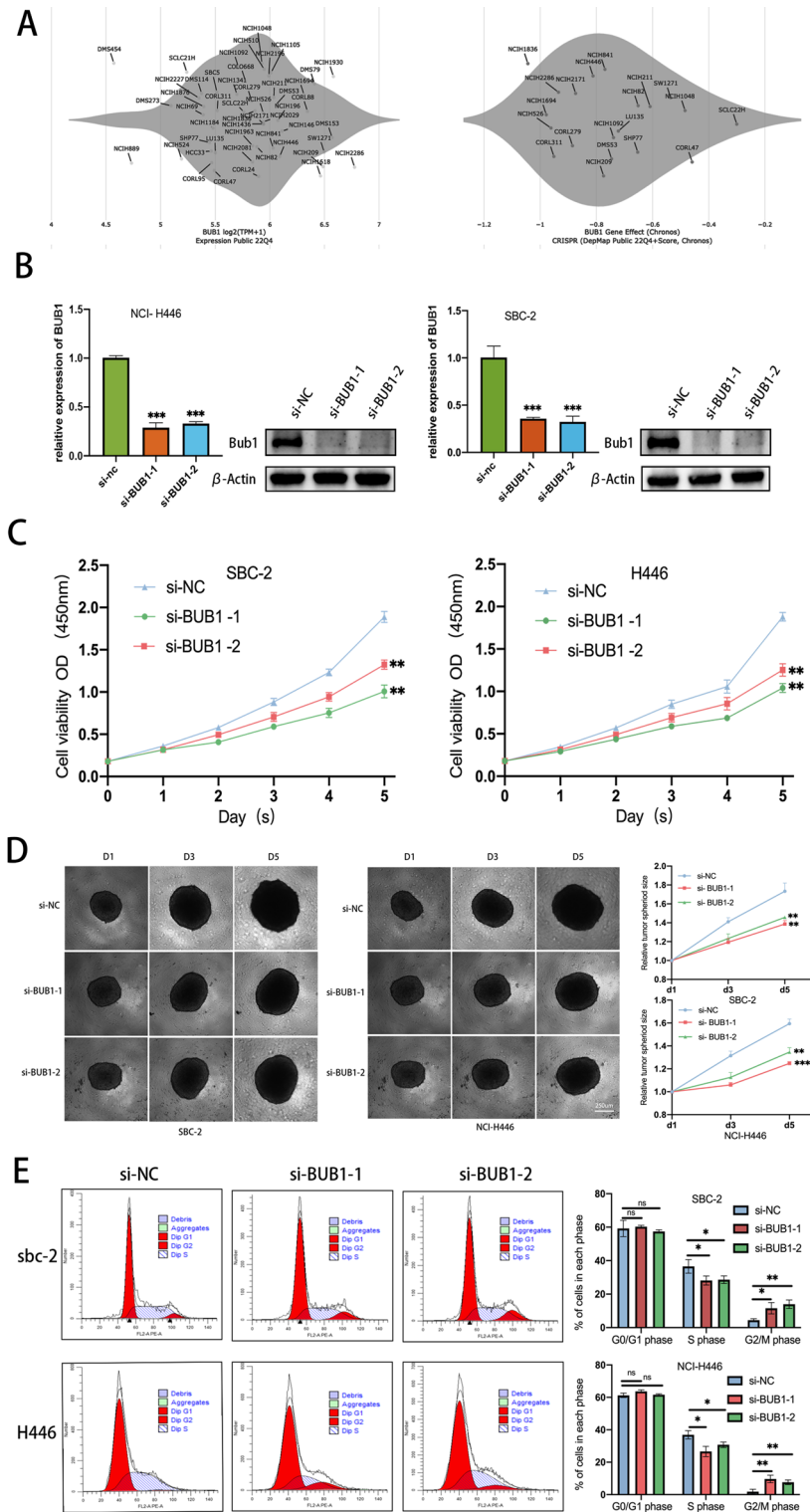


**Fig. 2.** In vitro analyses of the functional role of BUB1. **(A)** An overview of BUB1 expression in SCLC cell lines was conducted with the online DepMap tool. The BUB1 expression dataset is shown to the left. In contrast, the CRISPR dataset on the right demonstrates that BUB1 silencing impairs cell growth, with negative scores indicating slower growth following gene knockdown. In contrast, positive scores indicate more rapid growth after knockdown. Each gray dot corresponds to a particular cell line. **(B)** qPCR assessed BUB1 expression in NCI-H446 and SBC-2 cells following its siRNA-mediated silencing. And Western immunoblotting was utilized to confirm decreases in BUB1 protein content following its siRNA-mediated silencing. **(C)** For assessing the impact of BUB1 knockdown on tumor cell viability, CCK-8 tests were employed. **(D)** The effect of silencing BUB1 on tumor spheroid growth was measured. **(E)** The impact of BUB1 silencing on the cell cycle development in SBC-2 and NCI-H446 cells was evaluated using flow cytometry.



(siRNA-BUB1-1, siRNA-BUB1-2, siRNA-BUB1-3) were next evaluated for their ability to knock down BUB1 in SBC-2 and NCI-H446 cells. Both siRNA-BUB1-1 and siRNA-BUB1-2 significantly reduced BUB1 mRNA (Fig. 2B) and protein (Fig. 2B) levels in both cell lines compared to si-NC transfection. These constructs were thus selected for additional experimental use. Supporting the bioinformatics as mentioned above results, a CCK-8 experiment demonstrated that the viability of small cell lung cancer (SCLC) cells was significantly reduced after BUB1 knockdown (Fig. 2C) and increased with BUB1 overexpression (Supplementary Fig. 1A). Moreover, BUB1 knockdown hindered the development of tumor spheroids from SBC-2 and NCI-H446 (Fig. 2D).

Because BUB1 is crucial for mitotic processes<sup>17</sup>, a flow cytometry method was also used to evaluate how BUB1 knockdown affected the SBC-2 and NCI-H446 cells' ability to proceed through the cell cycle. In SCLC cells, BUB1 knockdown resulted in a significant increase in G2/M phase cells and a considerable drop in S phase cell frequency (Fig. 2E). This suggested that cell cycle arrest may be induced by BUB1 knockdown.

### BUB1 knockdown impairs the development of xenograft SCLC tumors in zebrafish

To directly validate the *in vivo* functions of BUB1, xenograft tumors were next implanted in zebrafish. BUB1-silenced and si-NC NCI-H446 and SBC-2 cells stained with a red fluorescent dye were injected into zebrafish yolk at 48 hpf. After a 48 h incubation period at 28 °C, the fluorescent tumor area in these animals was assessed via microscopy as a means of quantifying tumorigenesis (Fig. 3A). A significantly higher tumor growth rate was

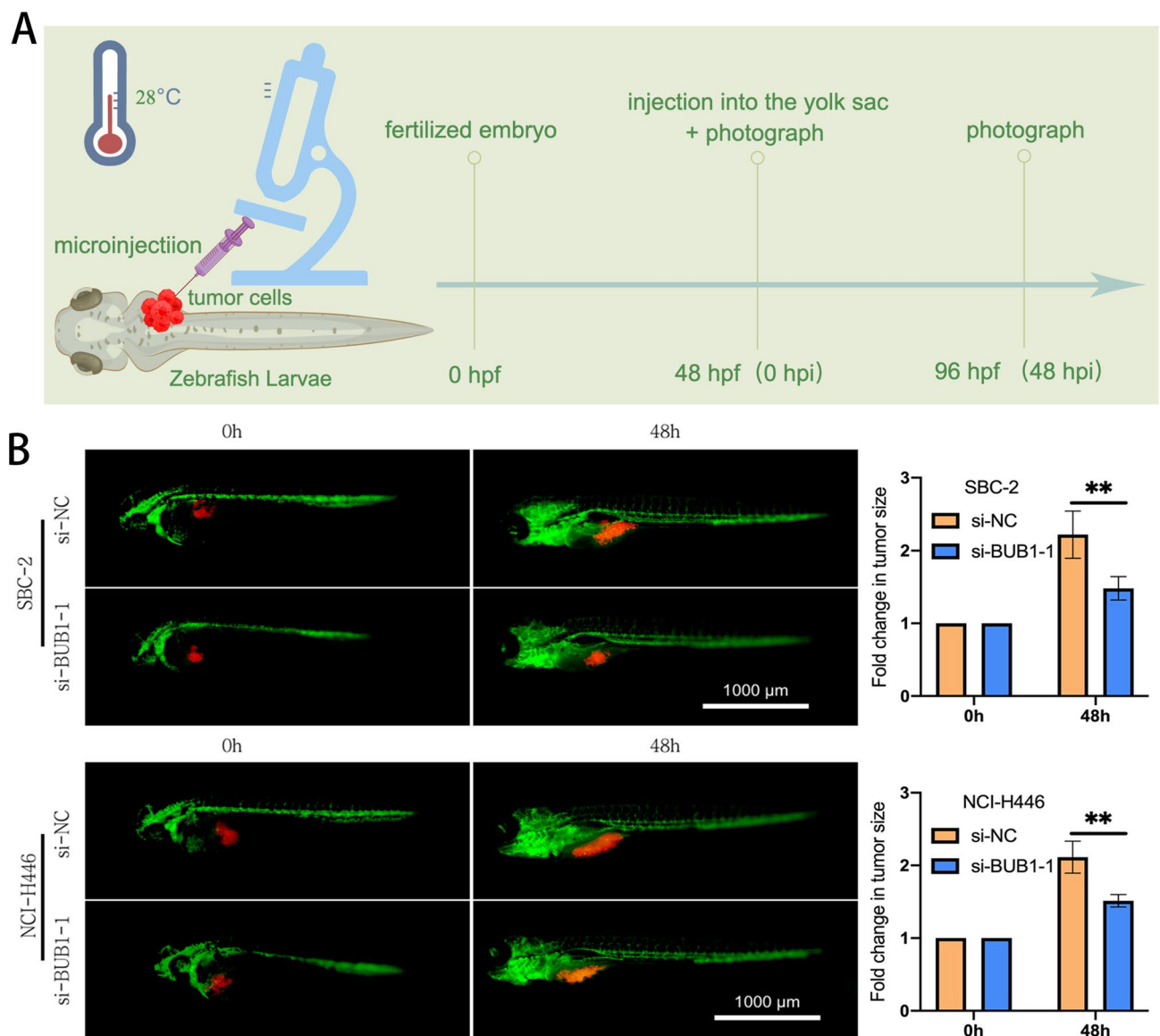


**Fig. 3.** Analyses of the *in vivo* functions of BUB1. **(A)** Schematic overview of the zebrafish xenotransplantation assay design used in this study. **(B)** The impact of si-BUB1 transfection on SCLC tumorigenesis in zebrafish, revealing a smaller fluorescent tumor area in the si-BUB1 group at 48 h relative to the control group. CM-Dil-stained SBC-2 and NCI-H446 cells are shown in red, while zebrafish vascular structures are shown in green. Results are provided as representative images and corresponding quantification.

detected in zebrafish that had been implanted with si-NC xenograft SCLC cells as compared to those injected with cells in which BUB1 had been knocked down (Fig. 3B). BUB1 silencing thus impaired *in vivo* SCLC tumorigenesis in zebrafish.

### BUB1 knockdown suppresses SCLC cell migratory and invasive activity

Since bioinformatics analyses suggested a potential link between BUB1 and distant metastasis, the impact of BUB1 on SCLC migratory activity was next assessed through a series of wound healing, 3D migration, and Transwell assay experiments. Knocking down BUB1 impaired wound healing activity at 24 and 48 h post-wounding (Fig. 4A). Additionally, BUB1 silencing resulted in a notable impairment of tumor sphere migration (Fig. 4B), whereas BUB1 overexpression significantly enhanced tumor sphere migration (Supplementary Fig. 1B). Transwell tests measuring the invasiveness of tumor cells further showed that BUB1 silencing was linked to markedly lower invasiveness in comparison to cells treated with si-NC (Fig. 4C). These data thus provide strong evidence that BUB1 knockdown can impair tumor cell invasivity and migration.

### Knockdown or overexpression of BUB1 alters EMT-associated protein expression

As BUB1 had a clear impact on the ability of SCLC cells to engage in migratory and invasive activity, Western immunoblotting was further employed to assess EMT-associated protein levels. SCLC cells with BUB1 knockdown had higher levels of the epithelial marker E-cadherin and lower mesenchymal markers (Vimentin, N-cadherin) and transcription factors (Snail, ZEB1) than control cells (Fig. 5). Conversely, BUB1-overexpressing SCLC cells displayed lower levels of the epithelial marker E-cadherin and higher levels of mesenchymal markers (Vimentin and N-cadherin) and transcription factors (Snail and ZEB 1) than control cells (Supplementary Fig. 2).

### BUB1 regulates the expression of proteins in the ATK/mTOR pathway

AKT/mTOR pathway activity has been closely tied to the viability, migration, and invasivity of tumor cells<sup>18</sup>. In this study, BUB1 silencing resulted in reduced levels of phosphorylated AKT and mTOR in SBC-2 and NCI-H446 cells, without any concomitant changes in total AKT or mTOR protein levels (Fig. 6). Conversely, overexpression of BUB1 led to increased levels of phosphorylated AKT and mTOR in the cells, again with no concurrent alterations in the total AKT or mTOR protein levels (Supplementary Fig. 2). Furthermore, treatment with the mTOR inhibitor everolimus reversed the effects of BUB1 overexpression on cell viability, tumor sphere migration, and the expression of proteins associated with the EMT in SCLC cells (Supplementary Fig. 1, 2).

### Effects of BUB1 pharmacological inhibition

A novel pharmacological inhibitor, BAY 1,816,032, has been shown to have anticancer effects by targeting BUB1<sup>15</sup>. The present study found that treatment with BAY-1816032 reduced both proliferation and migration in SCLC cells (Supplementary Fig. 3A, B). Additionally, the treatment led to an increase in the E-cadherin levels and a decrease in the levels of mesenchymal markers (Vimentin, N-cadherin) and transcription factors (Snail, ZEB1) in SCLC cells compared to untreated cells. Furthermore, inhibition of BUB1 kinase activity resulted in reduced phosphorylation of AKT and mTOR, although the concentrations of both proteins remained unaffected (Supplementary Fig. 3C). Moreover, to explore the effects of BUB1 pharmacological inhibition on normal lung epithelial cells, 16HBE cells were treated with BAY-1816032 and their proliferation and migration were assessed, finding that neither proliferation nor migration in epithelial cells were affected by BUB1 inhibition (Supplementary Fig. 3A, B).

## Discussion

SCLC is a highly aggressive type of cancer that tends to undergo early metastasis and readily acquire resistance to drugs<sup>19</sup>. SCLC incidence has been tied to several risk factors, including environmental pollution, occupational exposure, smoking, and genetic susceptibility. However, the precise molecular etiological basis for SCLC onset and progression is complex and remains incompletely characterized, underscoring a need to research these mechanisms to define more reliable therapeutic targets.

High levels of BUB1 expression have been reported in a wide array of cancer types, wherein it is associated with poor prognostic outcomes, influencing proliferative activity, metastasis, and a range of other processes<sup>20</sup>. The GEO dataset analyses performed herein consistently revealed high BUB1 expression levels in SCLC, as further confirmed through a series of qPCR, Western immunoblotting, and IHC analyses. This indicated that BUB1 is crucial in the development of SCLC. To test this possibility, BUB1 was knocked down using two siRNA constructs, revealing that the silencing of this gene profoundly impaired *in vitro* SCLC cell viability and proliferative activity while suppressing *in vivo* tumorigenesis in zebrafish. Wound healing, 3D migration, and Transwell assays additionally demonstrated that the loss of BUB1 was associated with the impairment of migratory and invasive activity, in line with prior data from osteosarcoma<sup>10</sup>, hepatocellular carcinoma<sup>11</sup>, and breast cancer<sup>21</sup>. These results thus confirmed the ability of high levels of BUB1 to serve as a tumor promoter in SCLC.

Cancer cells undergo rapid and persistent division such that they may exhibit greater SAC dependence than that observed for normal cells<sup>22</sup>. BUB1 is a critical component of the SAC<sup>23</sup> and is a vital regulator of the cell cycle<sup>24</sup>. In this study, flow cytometry revealed that BUB1 silencing higher the cell frequency in the G2/M phase, thus confirming that the loss of this SAC component was associated with cell cycle arrest at this checkpoint. However, no corresponding change in the frequency of G0/G1-phase cells was noted, and S-phase cells became less frequent. Small molecule drugs targeting the G2/M phase have been advanced as promising antitumor drugs for use alone or with radiotherapy<sup>25</sup>. The present results similarly support the relevance of BUB1 as a therapeutic target in SCLC.

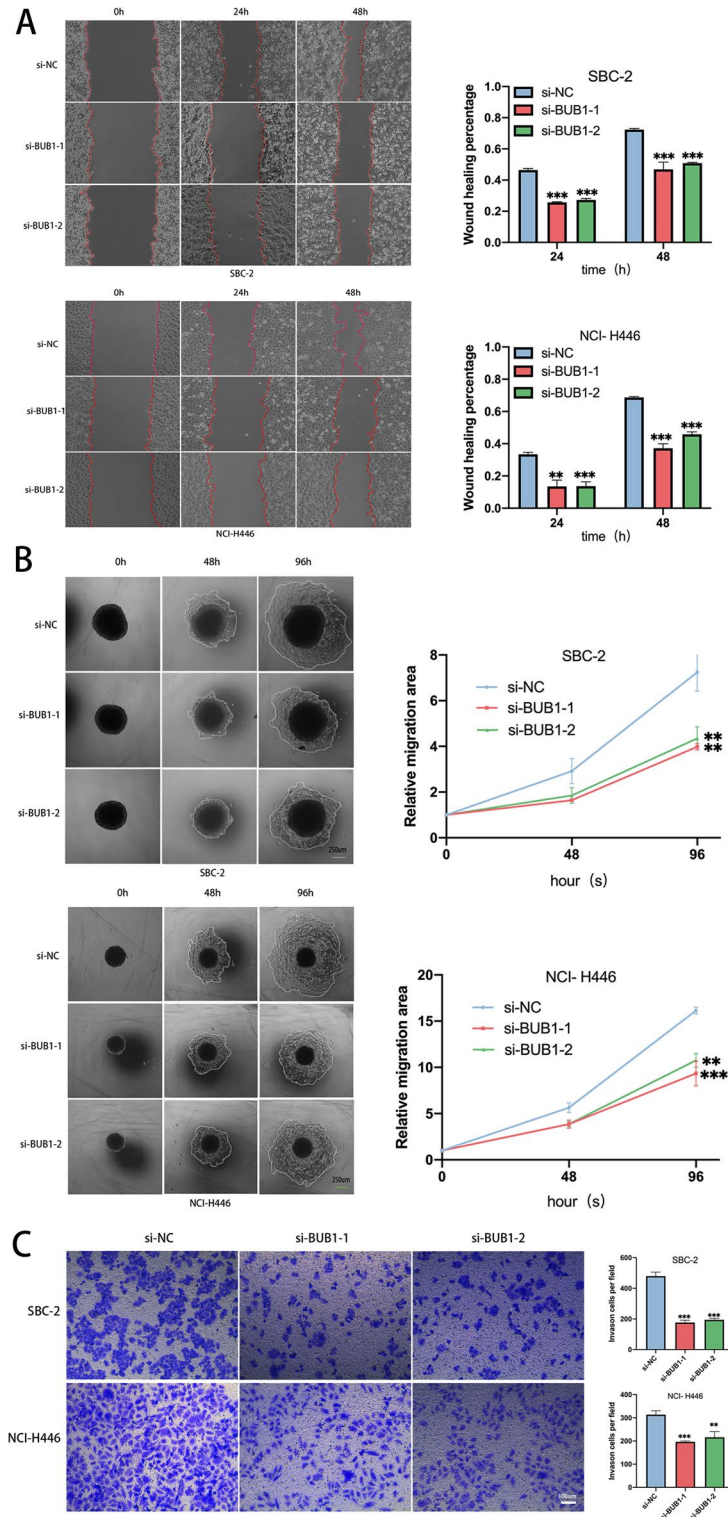


**Fig. 4.** BUB1 knockdown impairs SCLC cell invasive and migratory activity. **(A)** In a wound healing assay, BUB1 silencing resulted in the significant impairment of SCLC cell migratory activity. **(B)** The silencing of BUB1 inhibited the migration of SCLC cells on gelatin, as shown through the quantification of 3D migration assay data. **(C)** Transwell invasion assays and corresponding quantification.

The EMT is a complex process essential for the metastatic progression of many solid tumors, resulting in characteristic intracellular signaling reprogramming, the reorganization of the cytoskeleton, and a loss of cellular



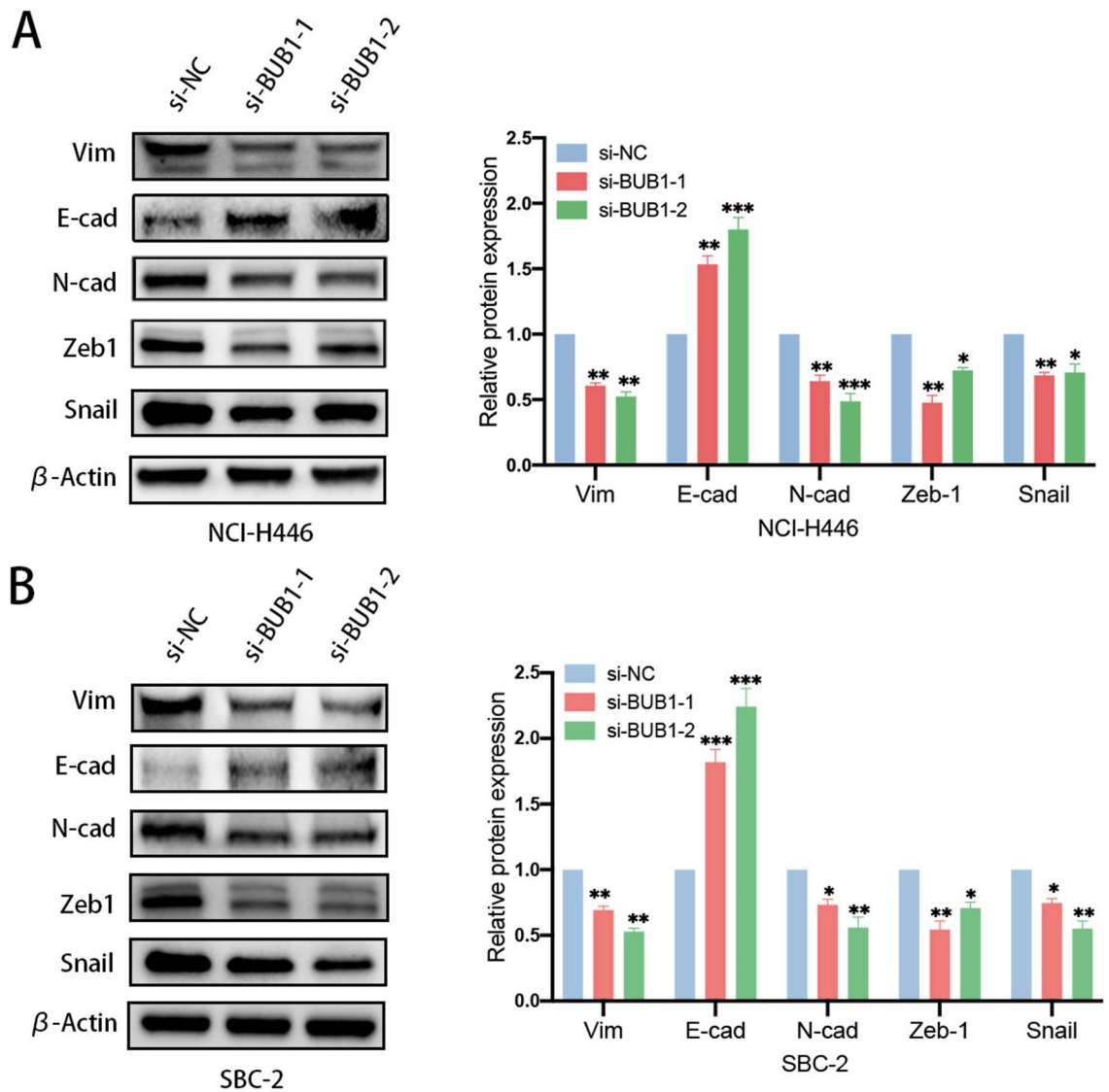


**Fig. 5.** EMT-associated proteins were assessed in NCI-H446 (A) and SBC-2 (B) cells following BUB1 knockdown. Protein extraction was carried out 48 h post-transfection. Representative blots are provided with the corresponding quantification.

polarity<sup>26,27</sup>. Another study observed that BUB1 is a critical mediator of TGF- $\beta$  signaling. This signaling pathway was impaired following the loss of BUB1 owing to changes in p38 MAPK and AKT signaling activity, ultimately damaging EMT induction<sup>28</sup>. Bioinformatics analyses revealed that higher BUB1 expression in SCLC patients was associated with higher M staging. Consistently, experimental investigations revealed that BUB1 silencing impaired the migratory and metastatic activity of SCLC cells, suggesting a possible role for BUB1 as a regulator of EMT activity in this cancer type. Consistently, analyses of EMT-related protein expression revealed significant reductions in ZEB1, Snail, N-Cadherin, and Vimentin levels following BUB1 silencing with a concomitant increase in E-cadherin levels in both NCI-H446 and SBC-2 cells. Conversely, the levels of ZEB1, Snail, N-Cadherin, and Vimentin were markedly increased in response to BUB1 overexpression, accompanied by a decrease in E-cadherin levels. Additionally, treatment with the mTOR inhibitor everolimus effectively counteracted the effect of BUB1 overexpression on the expression of EMT-associated proteins. As such, these data support a role for BUB1 in EMT induction in SCLC.

The AKT/mTOR pathway plays essential roles in regulating tumor cell proliferation and metastasis and shaping tumor-related neovascularization<sup>29,30</sup>. This signaling activity is also closely associated with EMT induction, promoting the activation of EMT-associated transcription factors while suppressing E-cadherin expression, culminating in EMT induction<sup>30</sup>. Abnormal AKT/mTOR signaling is frequently reported in SCLC, wherein it can promote phenotypic changes, distant metastasis, and other pro-malignant developmental processes<sup>30–32</sup>. SCLC tumors frequently acquire therapeutic resistance during treatment, and some studies have found that efforts to target the AKT/mTOR pathway can help overcome such resistance in this cancer type for both targeted and chemotherapeutic drugs<sup>33</sup>. AKT phosphorylation has been linked to the regulation of EMT activity in SCLC<sup>34</sup>. Subsequent investigations into the potential mechanisms by which BUB1 promotes the progression of SCLC

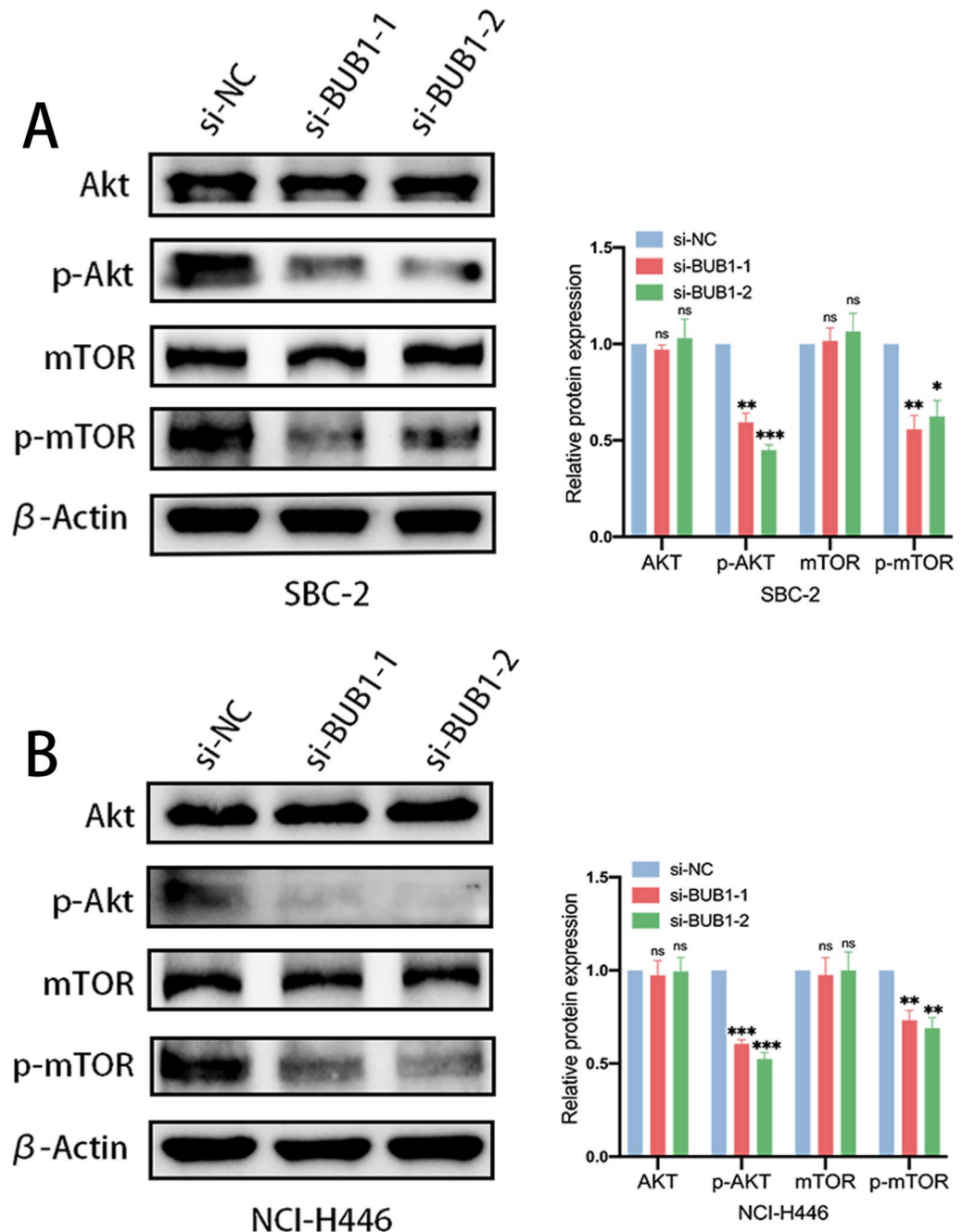


**Fig. 6.** AKT/mTOR pathway-associated protein levels following the siRNA-mediated knockdown of BUB1 within NCI-H446 (A) and SBC-2 (B) cells, with corresponding quantification. The protein extraction was performed 48 h post-transfection.

indicated that activation of the AKT/mTOR pathway was reduced after BUB1 silencing, while its activation was enhanced following BUB1 overexpression. This supports a model wherein BUB1 can induce the EMT process via AKT/mTOR signaling activation, ultimately driving the growth and metastatic progression of SCLC.

However, given that BUB1 knockdown altered the proportions of cells in different stages of the cell cycle, it is plausible to consider whether the phosphorylation status of mTOR and Akt is contingent upon the cell cycle. In this study, proteins were extracted 48 h after transfection. At this point, CCK-8 assays did not show any marked changes in cell proliferation, suggesting that changes in mTOR and Akt phosphorylation may precede alterations in cell cycle progression. This suggests that alterations in the phosphorylation status of mTOR and AKT may precede aberrations in cell cycle progression. Previous research has demonstrated the involvement of BUB1 in the regulation of osteosarcoma tumorigenesis, in part through the PI3K/AKT pathway<sup>10</sup>. Furthermore, multiple studies have suggested that the cell cycle serves as a central point for the AKT/mTOR signaling cascade<sup>35</sup>. Given

these findings, it is postulated that mTOR and AKT phosphorylation may not be cell-cycle dependent. Instead, BUB1 may affect the cell cycle through the AKT/mTOR pathway.

Investigating the effects of BAY-1816032 on SCLC cell models represents a promising research direction with potential clinical implications. Our results indicate that inhibition of BUB1 kinase activity mirrors the effects observed in SCLC cells following BUB1 knockdown, while having no significant effect on normal epithelial 16HBE cells, suggesting that these effects are specific for cells with elevated BUB1 expression. These findings suggest that pharmacological inhibition of BUB1 may hold promise for clinical applications.

This study is subject to certain limitations. Owing to limited sample availability, BUB1-associated survival data were not accessible for most patients, restricting prognostic analyses for this gene. Furthermore, further investigations are necessary to elucidate the underlying processes that connect BUB1 with the activation of the AKT/mTOR pathway and the induction of EMT.

## Conclusion

In summary, the present results revealed the pronounced upregulation of BUB1 in SCLC tumors and cell lines, wherein it was found to function oncologically, potentially enhancing EMT induction via the activation of AKT/mTOR signaling. BUB1 thus represents an attractive target for the treatment of SCLC.

## Data availability

The data that support the findings of this study are available from the corresponding author, Zhenhua Liu, upon reasonable request.

Received: 31 January 2024; Accepted: 29 August 2024

Published online: 04 September 2024

## References

- Wang, Q. *et al.* SCLC: Epidemiology, risk factors, genetic susceptibility, molecular pathology, screening, and early detection. *J. Thorac. Oncol.* **18**, 31–46 (2023).
- Rudin, C. M., Brambilla, E., Faivre-Finn, C. & Sage, J. Small-cell lung cancer. *Nat. Rev. Dis. Primers* **7**, 3 (2021).
- Kalemkerian, G. P. & Schneider, B. J. Advances in small cell lung cancer. *Hematol. Oncol. Clin. North Am.* **31**, 143–156 (2017).
- Horn, L. *et al.* First-line atezolizumab plus chemotherapy in extensive-stage small-cell lung cancer. *N. Engl. J. Med.* **379**, 2220–2229 (2018).
- Paz-Ares, L. *et al.* Durvalumab plus platinum-etoposide versus platinum-etoposide in first-line treatment of extensive-stage small-cell lung cancer (CASPIAN): A randomised, controlled, open-label, phase 3 trial. *Lancet* **394**, 1929–1939 (2019).
- Cheng, Y. *et al.* Effect of first-line serplulimab vs placebo added to chemotherapy on survival in patients with extensive-stage small cell lung cancer: The ASTRUM-005 randomized clinical trial. *JAMA* **328**, 1223–1232 (2022).
- Wang, J. *et al.* Adebrelimab or placebo plus carboplatin and etoposide as first-line treatment for extensive-stage small-cell lung cancer (CAPSTONE-1): A multicentre, randomised, double-blind, placebo-controlled, phase 3 trial. *Lancet Oncol.* **23**, 739–747 (2022).
- Biagioni, F. *et al.* miR-10b\*, a master inhibitor of the cell cycle, is down-regulated in human breast tumours. *EMBO Mol. Med.* **4**, 1214–1229 (2012).
- Jiang, N. *et al.* BUB1 drives the occurrence and development of bladder cancer by mediating the STAT3 signaling pathway. *J. Exp. Clin. Cancer Res.* **40**, 378 (2021).
- Huang, Z. *et al.* Inhibition of BUB1 suppresses tumorigenesis of osteosarcoma via blocking of PI3K/Akt and ERK pathways. *J. Cell. Mol. Med.* **25**, 8442–8453 (2021).
- Qi, W. B. *et al.* BUB1 predicts poor prognosis and immune status in liver hepatocellular carcinoma. *APMIS* **130**, 371–382 (2022).
- Mukherjee, A., Joseph, C., Craze, M., Chrysanthou, E. & Ellis, I. O. The role of BUB and CDC proteins in low-grade breast cancers. *Lancet* **385**, S72 (2015).
- Stahl, D. *et al.* Low BUB1 expression is an adverse prognostic marker in gastric adenocarcinoma. *Oncotarget* **8**, 76329–76339 (2017).
- Pagotto, S. *et al.* HNRNPL restrains miR-155 targeting of BUB1 to stabilize aberrant karyotypes of transformed cells in chronic lymphocytic leukemia. *Cancers (Basel)* **11**, 575 (2019).
- Siemeister, G. *et al.* Abstract 287: BAY 1816032 a novel BUB1 kinase inhibitor with potent antitumor activity. *Cancer Res.* **77**, 287–287 (2017).
- Vinci, M., Box, C. & Eccles, S. A. Three-Dimensional (3D) tumor spheroid invasion assay. *J. Vis. Exp.* **99**, 52686 (2015).
- Li, F. *et al.* The BUB3-BUB1 complex promotes telomere DNA replication. *Mol. Cell* **70**, 395–407 (2018).
- Sun, F. K. *et al.* Interleukin-8 promotes integrin  $\beta$ 3 upregulation and cell invasion through PI3K/Akt pathway in hepatocellular carcinoma. *J. Exp. Clin. Cancer Res.* **38**, 449 (2019).
- Rudin, C. M. *et al.* Molecular subtypes of small cell lung cancer: A synthesis of human and mouse model data. *Nat. Rev. Cancer* **19**, 289–297 (2019).
- Fujibayashi, Y. *et al.* Aberrant BUB1 overexpression promotes mitotic segregation errors and chromosomal instability in multiple myeloma. *Cancers* **12**, 2206 (2020).
- Han, J. Y., Han, Y. K., Park, G. Y., Kim, S. D. & Lee, C. G. Bub1 is required for maintaining cancer stem cells in breast cancer cell lines. *Sci. Rep.* **5**, 15993 (2015).
- Matthews, H. K., Bertoli, C. & de Bruin, R. A. M. Cell cycle control in cancer. *Nat. Rev. Mol. Cell Biol.* **23**, 74–88 (2022).
- Goto, Y. *et al.* Impact of novel miR-145-3p regulatory networks on survival in patients with castration-resistant prostate cancer. *Br. J. Cancer* **117**, 409–420 (2017).
- Chou, W. C., Cheng, A. L., Brotto, M. & Chuang, C. Y. Visual gene-network analysis reveals the cancer gene co-expression in human endometrial cancer. *BMC Genom.* **15**, 300 (2014).
- Yang, L. L. *et al.* Wee1 kinase inhibitor AZD1775 effectively sensitizes esophageal cancer to radiotherapy. *Clin. Cancer Res.* **26**, 3740–3750 (2020).
- Hu, X. H. *et al.* The RNA-binding protein AKAP8 suppresses tumor metastasis by antagonizing EMT-associated alternative splicing. *Nat. Commun.* **11**, 486 (2020).
- Pastushenko, I. & Blanpain, C. EMT transition states during tumor progression and metastasis. *Trends Cell Biol.* **29**, 212–226 (2019).
- Nyati, S. *et al.* The kinase activity of the Ser/Thr kinase BUB1 promotes TGF- $\beta$  signaling. *Sci. Signal.* **8**, ra1 (2015).

29. Cruickshanks, N. *et al.* Discovery and therapeutic exploitation of mechanisms of resistance to MET inhibitors in glioblastoma. *Clin. Cancer Res.* **25**, 663–673 (2019).
30. Peng, Y., Wang, Y. Y., Zhou, C., Mei, W. X. & Zeng, C. C. PI3K/Akt/mTOR pathway and its role in cancer therapeutics: Are we making headway?. *Front. Oncol.* **12**, 819128 (2022).
31. Krencz, I., Sztankovics, D., Danko, T., Sebestyen, A. & Khor, A. Progression and metastasis of small cell lung carcinoma: The role of the PI3K/Akt/mTOR pathway and metabolic alterations. *Cancer Metastasis Rev.* **40**, 1141–1157 (2021).
32. Li, X. F. *et al.* PI3K/Akt/mTOR signaling orchestrates the phenotypic transition and chemo-resistance of small cell lung cancer. *J. Genet. Genom.* **48**, 640–651 (2021).
33. Tsurutani, J., West, K. A., Sayyah, J., Gills, J. J. & Dennis, P. A. Inhibition of the phosphatidylinositol 3-kinase/Akt/mammalian target of rapamycin pathway but not the MEK/ERK pathway attenuates laminin-mediated small cell lung cancer cellular survival and resistance to imatinib mesylate or chemotherapy. *Cancer Res.* **65**, 8423–8432 (2005).
34. Zhao, L. M. *et al.* Flotillin1 promotes EMT of human small cell lung cancer via TGF- $\beta$  signaling pathway. *Cancer Biol. Med.* **15**, 400–414 (2018).
35. Li, H. *et al.* Small biomarkers with massive impacts: PI3K/AKT/mTOR signalling and microRNA crosstalk regulate nasopharyngeal carcinoma. *Biomark. Res.* **10**(1), 52 (2022).

## Acknowledgements

The authors would like to thank all the reviewers who participated in the review and MJEditor ([www.mjeditor.com](http://www.mjeditor.com)) for its linguistic assistance during the preparation of this manuscript.

## Author contributions

Z.H.L. and D.Y.L. designed the study. M.F.W. performed the study and wrote the paper. L.J.Y. and Y.F.H. conducted experiments. Z.X.S. participated in data analysis. All authors reviewed the manuscript.

## Funding

This work was supported by the Medical Innovation Project of Fujian((2016)300). Special Grant for Education and Scientific Research of Fujian Provincial Department of Finance (Fujian Finance Document (2021) 848).

## Competing interests

The authors declare no competing interests.

## Ethical approval

This study was authorized by the Ethics Committee of Fujian Provincial Hospital (Fuzhou, China). The patients or guardians signed an informed consent form before being enrolled in this study.

## Additional information

**Supplementary Information** The online version contains supplementary material available at <https://doi.org/10.1038/s41598-024-71644-4>.

**Correspondence** and requests for materials should be addressed to D.L. or Z.L.

**Reprints and permissions information** is available at [www.nature.com/reprints](http://www.nature.com/reprints).

**Publisher's note** Springer Nature remains neutral with regard to jurisdictional claims in published maps and institutional affiliations.

**Open Access** This article is licensed under a Creative Commons Attribution-NonCommercial-NoDerivatives 4.0 International License, which permits any non-commercial use, sharing, distribution and reproduction in any medium or format, as long as you give appropriate credit to the original author(s) and the source, provide a link to the Creative Commons licence, and indicate if you modified the licensed material. You do not have permission under this licence to share adapted material derived from this article or parts of it. The images or other third party material in this article are included in the article's Creative Commons licence, unless indicated otherwise in a credit line to the material. If material is not included in the article's Creative Commons licence and your intended use is not permitted by statutory regulation or exceeds the permitted use, you will need to obtain permission directly from the copyright holder. To view a copy of this licence, visit <http://creativecommons.org/licenses/by-nc-nd/4.0/>.

© The Author(s) 2024